Geological Quarterly, 2019, **63** (3): 493–504
DOI: http://dx.doi.org/10.7306/gq.1483

In situ gamma-ray measurements of ^{40}K, ^{232}Th and ^{238}U in high-grade metamorphic rocks from the Sowie Mountains (Sudetes, SW Poland)

Dariusz MALCZEWSKI[1, *] and Jerzy ŻABA[1]

[1] University of Silesia, Faculty of Earth Sciences, Będzińska 60, 41-200 Sosnowiec, Poland

Malczewski, D., Żaba, J., 2019. *In situ* gamma-ray measurements of ^{40}K, ^{232}Th and ^{238}U in high-grade metamorphic rocks from the Sowie Mountains (Sudetes, SW Poland). Geological Quarterly, **63** (3): 493–504, doi: 10.7306/gq.1483

Associate editor: Stanisław Wołkowicz

This paper reports on the abundance of primordial radionuclides (^{40}K, ^{232}Th and ^{238}U) in characteristic lithologies from the Sowie Mountains (SW Poland). *In situ* gamma-ray measurements were conducted at 12 localities hosting exposed augen gneiss, flaser gneiss, granulite, homophanized gneiss, hornblendite, layered gneiss, layered migmatite, migmatic gneiss, mylonitic gneiss and mylonitic granulite. The activity concentration of ^{40}K varied from 180 Bq kg^{-1} (mylonitic granulite) to 845 Bq kg^{-1} (layered gneiss). The activity concentrations associated with ^{228}Ac (^{232}Th) varied from 10 Bq kg^{-1} (mylonitic granulite) to 53 Bq kg^{-1} (homophanized gneiss), while activity associated with ^{226}Ra (^{238}U) varied from 9 Bq kg^{-1} (mylonitic granulite) to 43 Bq kg^{-1} (layered gneiss). An augen gneiss adjacent to the Intra-Sudetic Fault showed the highest combined Th + U activity (89 Bq kg^{-1}). The average Th/U ratio (3.6) calculated for gneiss outcrops of the Sowie Mountains falls within the range reported for biotite gneiss (3.5–4). Subsurface outcrops from the Walim–Rzeczka underground complex did not give noticeably higher ^{238}U activities. The results obtained for the Sowie lithologies are compared with those obtained by similar methods for similar rocks as reported in literature sources.

Key words: gneisses, Sowie Mountains, Sudetes, natural radioactivity, *in situ* measurements.

INTRODUCTION

The Sowie Mountains (Sowie means “owl” in English) are located in southwestern Poland (Fig. 1) and constitute a part of the Sowie Mountain block (Sowie Mountains gneiss massif, after Żelaźniewicz et al., 2011). The block constitutes a major geological unit in the Western Sudetes, which lie along the northeast margin of the Bohemian Massif and represent an internal part of the Variscan Orogen. Cwojdziński (1980) interpreted the Sowie Mountain block as representing a micro-continent. Quenardel et al. (1988), Matte et al. (1990), Cymerman et al. (1997) and Aleksandrowski and Mazur (2002) suggest that it represents a terrane or a terrane fragment. Aleksandrowski and Mazur (2002) assigned the area to the Sowie Mountains–Kłodzko tectonostratigraphic terrane.

The Sowie Mountains themselves are surrounded by faults and span two geologically distinct provinces or sectors separated by the Sudetic Marginal Fault. The eastern unit of the Sowie Mountains resides within the Fore-Sudetic Block, while a horst or uplifted western unit lies within the Sudetic Block (Fig. 1). To the north of the mountains lies the Świebodzice Fold Structure, and to the south and south–west lie the Bardo Fold Structure and Intra-Sudetic Synclinorium, respectively. However, the Intra-Sudetic Fault separates the Sowie Mountains from these structures (Fig. 1). The Fore-Sudetic Block, which runs along the Sudetic Marginal Fault, forms the Sowie’s northeastern border (Fig. 1).

The Sowie Mountains (Fig. 2) consist primarily of gneiss exhibiting considerable variation in fabric and mineralogy (e.g., Polański, 1955; Grocholski, 1968; Kryza, 1981; Żelaźniewicz, 1987). Laminated gneiss, scaly (flaky) gneiss, layered gneiss, flaser (streaky) gneiss and augen gneiss comprise the most common varieties (Fig. 1). The lithologies frequently exhibit gradational mineralogy and fabric. The less common aplitoid gneiss, massive gneiss, veined gneiss, coarse-lensoid gneiss and nodular gneiss (Kryza, 1981; Żelaźniewicz, 1987) occur locally in certain areas.

This study conducted *in situ* measurements of ^{40}K, ^{232}Th and ^{238}U activity concentrations in the Sowie Mountain units. The data represent novel measurements for the study area and were compared with similar data reported in literature sources from other locations. Our discussion and interpretations explore the possibility and potential constraints of using gamma-ray measurements to determine protoliths and detect other geological processes that may influence K, Th and U concentrations.

* Corresponding author, e-mail: dariusz.malczewski@us.edu.pl

Received: May 21, 2018; accepted: May 23, 2019; first published online: August 23, 2019

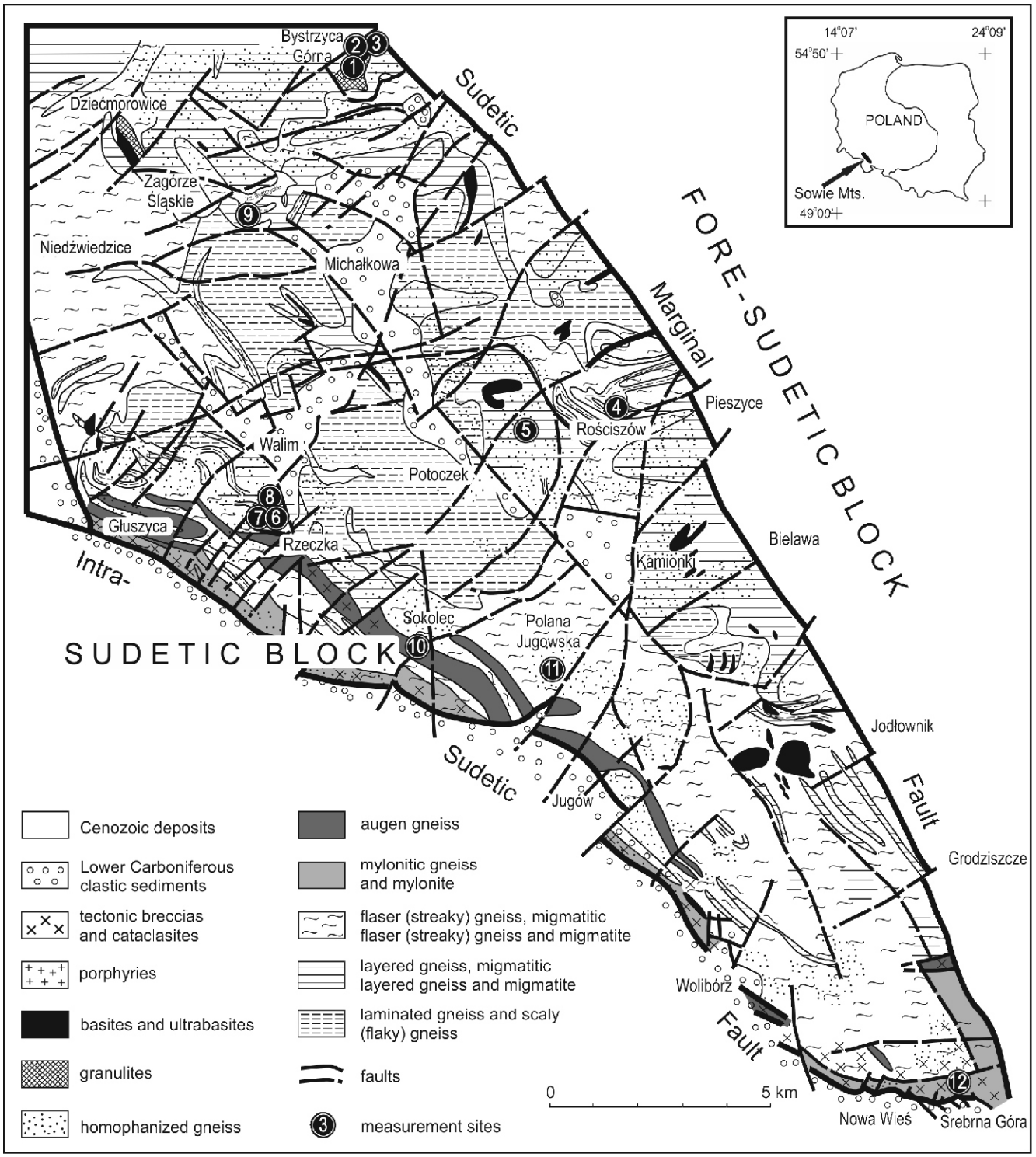

Fig. 1. Geological map of the Sowie Mountains showing measurement localities (modified and supplemented after Polański, 1955; Grocholski, 1967, 1968; Żelaźniewicz, 1987; Oberc et al., 1994)

GEOLOGICAL SETTING

Homophanized gneiss occurs throughout the Sowie Mountains (Grocholski, 1967; Żelaźniewicz, 1987). It generally forms from advanced static recrystallization of different textural types of gneiss, namely flaser (streaky), layered and laminated varieties. The degree of homophanization (blurring of older directional structures) varies significantly. Gneiss from the Sowie Mountains that experienced the greatest degree of homophanization (Mehnert, 1971) resembles granite.

Other types of gneiss appear highly migmatized. Migmatic gneiss and migmatite occur throughout the study area, especially in the northern part of the Sowie Mountains. In spite of their migmatitic character, original gneissic fabrics remain in evidence, making it possible to identify parent material.

Fig. 2. A view of the Sowie Mountains from the north

Nearly all the textural varieties of migmatite proposed by Mehnert (1968) occur in the Sowie Mountains. Mehnert differentiated the following migmatite textures based on the distribution of melanosome and leucosome material: agmatic, diktyonitic, schollen (reft), phlebitic (rein), stromatic (layered), surreitic, ptygmatic folded, ophthalmic (augen), stictolithic (fleck), schlieren, and nebulic (Grocholski, 1967; Kryza, 1981). To simplify the classification, Kryza (1981) suggested that the migmatite from the Sowie Mountains consists of two major groups: phlebites represented by layered and veined migmatite, and nebulites represented by highly homophanous migmatite, which include abundant, apparently leucocratic material. Minor melanosome appears only in the form of streaks, schlieren, loafy rafts or faint ghost structures. Migmatite generally consists of quartz and plagioclase (An_{30-40}) with subsidiary biotite and local microcline, garnet and muscovite.

Deformation transformed the gneiss from the Sowie Mountains into mylonitic gneiss and mylonite. Mylonite appears in major fault zones (Fig. 1) including the Intra-Sudetic Fault (Grocholski, 1968; Żelaźniewicz, 1987; Aleksandrowski et al., 1997) where it occurs in greatest abundance. Fault zones typically host multi-stage gneissic tectonic breccia (Grocholski, 1968; Pacholska, 1978; Żelaźniewicz, 1987; Oberc et al., 1994) as well as cataclasite and gneiss cataclized to varying degrees. Tectonic breccias cover large portions of the southern Sowie Mountains block (Fig. 1).

The gneiss exhibits two predominant mineral assemblages: biotite-oligoclase-quartz and two-mica-oligoclase-quartz (Kryza, 1981). Some gneiss and the migmatite from the Sowie Mountains also include significant proportions of microcline, sillimanite or cordierite making it possible to distinguish certain lithologies such as microcline gneiss and migmatite, sillimanite (mostly fibrolite) gneiss and migmatite or cordierite gneiss and migmatite. Many varieties of Sowie gneiss and migmatite contain a tiny amount of garnet. Other accessory minerals include apatite, monazite, zircon and Fe-oxides.

Granulites and basites represent subordinate lithologies among the Sowie gneiss and migmatite. These lithologies also include relatively minor occurrences of ultrabasites, crystalline limestones, calc-silicate rocks, small felsic intrusive bodies, pegmatite dikes and porphyries.

Granulite occurs to a very limited extent in several northerly locations in the Sowie Mountains, including the vicinity of Bystrzyca Górna and Zagórze Śląskie (Fig. 1). This granulite exhibits light coloured, fine-grained textures composed of quartz, oligoclase, alkali feldspar, garnet and kyanite with accessory rutile, apatite, zircon and opaque minerals. Units show either no foliation or perfect foliation, the latter being mainly due to the occurrence of banded quartz grains and directional orientation of darker minerals, especially biotite (Polański, 1955; Kryza, 1981; Żelaźniewicz, 1985, 1987; Kryza et al., 1996; O'Brien et al., 1997, Kryza and Fanning, 2007). The units in the vicinity of Bystrzyca Górna host piribolites, an unusual lithology that consists of green hornblende, diopside, garnet and plagioclase. This lithology formed from regional metamorphism of granulite facies.

Basites consist of amphibolites and hyperites (Fig. 1). Amphibolites appear as diverse lithologies including para-amphibolites with crystalline limestone intercalations and ortho-amphibolites, which still contain relics of primary igneous rocks. Amphibolites consist mostly of hornblende and plagioclase with varying proportions of quartz and garnet. They may also contain subordinate biotite, pyroxene, carbonate, titanite, apatite and ore-type minerals (Polański, 1955; Grocholski, 1967; Kryza, 1981). Hyperite from the Sowie Mountains occurs as intrusive bodies (veins and stems) that discordantly cut through gneiss and migmatite in the vicinity of Dziećmorowice, Walim and Rościszów (Grocholski, 1967).

Ultrabasite occurs mainly in the northerly areas of the Sowie Mountains, near Bystrzyca Górna and Zagórze Śląskie (Fig. 1) where it intrudes gneiss and granulite (Żelaźniewicz, 1985). Ultrabasite includes peridotite, pyroxenite, apatite-bearing hornblendite, hornblendite with olivine, lherzolite, websterite, harzburgite and dunite, along with saxonite and serpentinite formed *in situ* (Sachanbiński, 1973; Bakun-Czubarow, 1981; Narębski et al., 1982; Janeczek et al., 1994; Gunia, 1997; Winchester et al., 1998; Kryza and Pin, 2002).

Crystalline limestone is generally scarce in the Sowie Mountains but it does occur as small lenticular intercalations (up to ~40 cm thick) within amphibolite and gneiss near Bielawa and Zagórze Śląskie (Grocholski, 1967; Kryza, 1981). Intrusive granitoids form small bodies (up to 1 m across) emplaced along the foliation planes of adjacent gneiss. Intrusions exhibit medium-grained textures consisting of quartz, oligoclase and microcline with subordinate muscovite and sillimanite plus rare biotite.

The crystalline basement of the Sowie Mountains nonconformably underlies middle (Fig. 1) and Upper Visean sedimentary units with abundant marine fossils (Żakowa, 1966). These units include sedimentary breccia, conglomerate, shale, greywacke shale and sandstone. Lower Namurian (Grocholski, 1967) conglomerates and sandstones occur locally within grabens. These graben structures also preserve other isolated occurrences of Paleozoic deposits. Carboniferous units covered the area prior to the Miocene uplift of the Sowie Mountain block.

Gneiss and migmatite represent ~95% of the Sowie massif outcrops. Their chemistry and mineralogy, along with intercalations of crystalline limestone and calc-silicate rocks, unequivocally demonstrate a sedimentary origin for most of the gneissic and amphibolite lithologies from the Sowie Mountains (Polański, 1955; Kryza, 1981; Żelaźniewicz, 1987). Some lithologies, such as the augen gneiss, may represent deformed granitic igneous protoliths (e.g., Polański, 1955). However, Grocholski (1967) interpreted these units as paragneiss. Augen gneiss typically forms narrow elongate bodies running parallel to the Intra-Sudetic Fault along the southwestern margin of the Sowie Mountains (Fig. 1). Some amphibolites may have been derived from magmatic protoliths. Sowie Mountain protoliths, however, consist mostly of psammitic to pelitic sources interpreted to have consisted of fine to medium-grained sandy to muddy greywackes locally enriched with clay material (Polański, 1955; Kryza, 1981; Gunia, 1999). These formed within a Neoproterozoic-Cambrian basin intruded by granitic plutons between 490 and 480 Ma (Żelaźniewicz et al., 2011). Metamorphism of these units reached upper amphibolite grade and occurred from 385–370 Ma (Van Breemen et al., 1988; Bröcker et al., 1998). From the Late Silurian to Early Devonian, a granulite slab formed earlier, probably from Cadomian continental crust, subducted beneath the Variscan Belt to mantle depths (Pin and Vielzeuf, 1983; Vielzeuf and Pin, 1989). This convergent tectonism, associated with Middle to Late Devonian collision (Aleksandrowski and Mazur, 2002), caused high pressure, high temperature metamorphism (Kryza et al., 1996; Kryza and Fanning, 2007). The uplift of the Sowie Mountains gneissic complex, which may have formed as early as 370–360 Ma, shifted the complex from upper amphibolite facies temperatures into greenschist zone conditions. Exhumation was relatively rapid and occurred due to a tectonic inversion towards the end of the Devonian at 360 Ma (Van Breemen et al., 1988; Kryza and Fanning, 2007).

The Sowie Mountain structures suggest multiple phases of tectonism (e.g., Grocholski, 1967; Żelaźniewicz, 1987). Five tectonic episodes accompanied by medium and high grade metamorphism occurred prior to the Late Devonian. Deformation episodes include mainly Barrovian-type metamorphism (Żelaźniewicz, 1987; Van Breemen et al., 1988). Accordingly, Sowie Mountain gneiss shows five generations of folds and accompanying structures formed under different deformational conditions. Multi-stage fault systems form a fine net across the Sowie Mountains, accompanied by tectonic breccias of various ages, cataclasite and mylonite. Most faults trend in a NW–SE or NE–SW direction. The NE–SW faults show significant dispersion of directions from WSW–ENE to NNE–SSW. A significant proportion of the young faults formed during the Miocene uplift of the Sowie Mountains, which resulted in the formation of numerous horst and graben structures that were subsequently filled with clastic sediments derived from Lower Carboniferous units (Fig. 1).

METHODS, MATERIALS, AND SITE LOCATIONS OF *IN SITU* MEASUREMENTS

We measured in situ gamma-ray emissions at 12 sites throughout the study area.

Site 1 was a road-cut located north-east of the Bystrzyca Górna railway station (Fig. 1, point 1; Fig. 3A) excavated for the railway line (Janeczek et al., 1994). This site includes granulite exposed along the northwestern slope of the excavation where it spans a few tens of metres in length and reaches 4 m in height. The granulite exhibits perfectly developed foliation. Pin and Vieizeuf (1983) refer to these units as “type I granulite” and interpret them as derived from continental crust subducted in the Variscan Belt to mantle depths at ~400 Ma (Vielzeuf and Pin, 1989; Kryza and Fanning, 2007). The unit exhibits fine-grained textures consisting primarily of quartz, oligoclase, potassium feldspar, garnet and directionally oriented sheets of secondary biotite, and there are signs of ductile shearing.

Site 2 was located in Bystrzyca Górna a few tens of metres north-east of site 1 (Fig. 1, point 2; Fig 3B). A northwestern slope of the excavation west of the Bystrzyca Górna railway station exposes a chaotically structured ultramafite represented by an apatite-bearing hornblendite (Janeczek et al., 1994). The outcrop occurs beneath a bridge along the Świdnica–Zagórze Śląskie road and runs for a few hundred metres with heights of 2 to 3 m. The hornblendite consists of idiomorphic crystals of hastingsitic hornblende that reach lengths of up to 20 cm, along with abundant interstitial apatite (up to 5 cm in diameter). Due to its coarse-grained texture, this unit has often been referred to as a hornblende pegmatite (Sachanbiński, 1973). The textural features of the rock, however, technically categorize it as an adcumulate. Numerous zones of brecciation and mylonitization appear within the hornblendite, outlining at least two stages of brittle deformation (Janeczek et al., 1994). Secondary biotite, formed as a result of hornblende biotization, occurs locally in hornblendite near shear zones. These domains locally contain small amounts of quartz (Janeczek et al., 1994). Hornblendite and other ultrabasites from the Sowie Mountains and surrounding areas comprise a major component of a Late Devonian ophiolitic complex (e.g., Narębski et al., 1982; Żelaźniewicz, 1987).

Site 3 was also located in Bystrzyca Górna less than 20 m north-east of site 2 (Fig. 1, point 3; Fig. 3C). It occurs along the south-east slope of the railway excavation and consists of an outcrop a dozen metres in length and up to 3 m high. Mylonitic granulite forms around the margins of a granulite body containing granulite intercalations (ultramafites). The rocks of this outcrop formed in a ductile shear zone that exhibits overthrust characteristics probably related to tectonic emplacement of a granulitic slab within the neighboring Sowie gneiss. Mylonitic granulite is characterized by a distinctive foliated texture making it similar to layered-laminated gneiss.

Site 4 was located near the center of Rościszów village along the left bank of the Kłomnica River at the foot of Głodówka Mountain (Fig. 1, point 4; Fig. 3D). Measurements were performed on the lower part of a large boulder several metres high and ~40 m long. The boulder consists of strongly folded migmatitic layered gneiss exhibiting occasional homophanization features that caused local, irregular blurring of the original directional structure. This example of float corresponds to

Fig. 3. Photos of site locations and detector set-up

A – location 1 (Bystrzyca Górna, granulite); **B** – location 2 (Bystrzyca Górna, hornblendite); **C** – location 3 (Bystrzyca Górna, mylonitic granulite); **D** – location 4 (Rosciszów, migmatic layered gneiss); **E** – location 5 (Potoczek, homophanized gneiss); **F** – location 6 (Walim–Rzeczka complex, migmatic layered gneiss); **G** – location 7 (Walim–Rzeczka complex, layered gneiss); **H** – location 8 (Walim–Rzeczka complex, layered gneiss); **I** – location 9 (Zagórze Śląskie, layered migmatite); **J** – location 10 (Sokolec, augen gneiss); **K** – location 11 (Jugów, flaser gneiss); **L** – location 12 (Srebrna Góra, mylonitic gneiss)

biotite-oligoclase-quartz gneiss observed in the outcrop. The gneiss investigated forms a narrow zone within dispersed scaly (flaky) gneiss.

Site 5 was located in the eastern part of Potoczek village at the foot of Maria Mountain, along the left bank of the Kłomnica River (Fig. 1, point 5; Fig. 3E). Measurements were conducted on the upper sections of the outcrop that consist entirely of homophanized gneiss. The outcrop analyzed showed numerous folds with local original directional fabrics. The mineral composition corresponds to biotite-oligoclase-quartz gneiss containing abundant and sizeable biotite enclaves, which locally form biotite gneiss.

Site 6 was located in the southern part of the town of Walim between the town center and Rzeczka village (Fig. 1, point 6; Fig. 3F). Measurements were performed on a boulder found on the left bank of the Walimka River along the northeastern slope of Góra Ostra (Ostra Mountain). The sample locality was situated a few metres from the entrance to the No. 2 tunnel of the Walim–Rzeczka underground complex that was excavated by forced labor under the Nazis during World War II as part of Project Riese. The boulder is ~9 m high, and 10 m wide and it hosts migmatitic layered gneiss. These rocks show homophanization features, corresponding to biotite-oligoclase-quartz gneiss, that obscure directional fabrics. Some parts of the boulder contain a large amount of biotite, designating them as biotite gneiss. The boulder is cut by medium-grained, phaneritic veins of granite reaching up to 1 m in thickness. The veins are aligned with the steeply inclined foliation of the gneiss.

Site 7 occurred within tunnel No. 2 of the Walim–Rzeczka underground complex, ~90 m from the entrance in a large un-

derground hall that is 10 m wide and over a dozen metres high (Fig. 1, point 7; Fig. 3G). This tunnel and hall expose strongly folded gneiss and the hall contains a large debris fall formed from the collapse of a ventilation shaft excavated in a fault zone. The No. 2 tunnel specifically intersects a sinistral strike-slip fault displacing a muscovite-bearing pegmatite vein of several centimetreswidth. The site includes typical layered biotite-oligoclase-quartz gneiss with significant amounts of biotite and biotite schist intercalations. Bodies of medium-grained, phaneritic felsic material intrude the gneiss in the hall.

Site 8 was the Walim–Rzeczka complex outcrop at the No. 2 tunnel face, 125 m from the tunnel entrance (Fig. 1, point 8; Fig. 3H). The tunnel ends in a huge, 110 10 15 m hall located deep within the massif. Rock debris covers the southwestern side of the hall. The face of tunnel No. 2 consists of typical folded, layered, biotite-oligoclase-quartz gneiss.

Site 9 was located in Zagórze Śląskie along the southern shore of the Bystrzyca reservoir (Jezioro Bystrzyckie) near Michałkowa village (Fig. 1, point 9; Fig. 3I). A local road runs along outcrops reaching 4 m high and 35 m long. The outcrop consists of layered migmatite of stromatite character (after Mehnert's classification, 1968). The simplified classification scheme suggested by Kryza (1981) defines these lithologies as phlebite. The units formed as a result of migmatization of the layered biotite-oligoclase-quartz gneiss commonly occurring in the area.

Site 10 was located in Sokolec village along the left bank of the Sowie Potok (Fig. 1, point 10; Fig. 3J). Outcrops here host units characteristic of the western slope of Grabina Mountain (so called Czarny Stok) above the road from Rzeczka to Sokolec. The outcrop investigated was 5.5 m high and ~10 m long consisting of augen gneiss transitioning into flaser (streaky) gneiss. This gneiss occurs in a narrow NE–SW trending zone running parallel to the Intra-Sudetic Fault (Fig. 1). The mineral composition of this gneiss differs notably from that of other Sowie gneiss. The former is typically a strongly cataclized two mica-microcline gneiss that includes plagioclase, quartz, biotite, abundant muscovite and microcline forming augens up to several centimetres in diameter. The majority of the outcrop that was analysed consists of fine augen gneiss exhibiting signs of sinistral shearing. The appearance of S-C type features, sigma-type augens and occasional delta-type augens indicates some degree of deformation under ductile conditions. Polański, (1955) originally interpreted these units as orthogneiss but later researchers identified evidence of sedimentary protoliths (Grocholski, 1967; Kryza, 1981). The augen gneiss is cut by numerous small veins of pegmatite containing columns and needles of black tourmaline.

Site 11 was near Jugów village, beneath Polana Jugowska (Jugów Glade) where the vast Grabina–Koziołki–Kozia Równina massif hosts flaser (streaky) gneiss showing differing degrees of homophanization (Fig. 1, point 11, Fig. 3K). Measurements were performed on a 4.5 m high outcrop extending ~13 m in length above the local road running through Przełęcz Jugowska (Jugów Pass) and connecting Sokolec to Kamionki. This locality hosts two types of mica-oligoclase-quartz gneiss that appear light in colour and exhibits well developed flat-parallel foliation. Varying degrees of homophanization obscure pre-existing directional structures.

Site 12 sampled a zone of mylonitic gneiss and mylonite within the upper Warowna Góra in Srebrna Góra village (Fig. 1, point 12; Fig 3L). Measurements were performed on an outcrop along the northern embankment of an old moat beneath Fort Wysoka Skała (also known as Fort Rogowy which is a part of the 18th century Prussian fortress "Twierdza Srebrnogórska"). The outcrop reaches 10 m high and 7 m long and it hosts migmatic gneiss and migmatite. Fabrics in these units show close correspondence with the multiphase activity of the Intra-Sudetic Fault, which runs along the foot of Warowna Mountain near Przełęcz Srebrna (Srebrna Pass). The locality also includes breccias, formed by several stages of tectonic activity, and cataclasite. Along with the gneiss and migmatite, these units were developed on the previously formed layered and flaser (streaky) gneiss.

In situ gamma-ray measurements were performed using a portable *GX3020* gamma-ray spectrometry workstation (Fig. 3) during the fall of 2009 and spring of 2010. The *GX3020* system (Canberra Industries) consists of a coaxial *HPGe* detector (32% efficiency) with a cryostat mounted on a tripod, a multichannel buffer (*InSpector 2000 DSP*), and a laptop. The detector bias was 4000 V and the energy resolution was 0.86 keV at 122 keV and 1.7 keV at 1.33 MeV. The detector was mounted in both horizontal and vertical (site 5) orientations 0.2–1 m from the outcrops surface at 0.5-1.2 m height above the ground. These geometries capture a majority of emitted gamma-rays from a 2–10 m radius area (Helfer and Miller, 1988). The detector samples emission depths of several tens of cm depending on lithology and photon energy. The total duration of a single measurement conducted at each location was two hours and *in situ* object counting software (ISOCS) was used for calibration efficiency. The *ISOCS* procedure requires the use of the *Geometry Composer in Genie 2000 v.4*. The *Geometry Composer* parameters that must be specified include outcrop dimensions, the rock type, and the distance between the rock outcrop and the detector. The final output from the *ISOCS* software is the full energy efficiency for a given rock-detector geometry. The "Well" template from the *Geometry Composer* package was used to perform the efficiency calibration and activity determination for samples from sites 7 and 8. Dimensions of height, width, and length of the tunnels along with the detector position were specified as required by the template.

The apparatus and software quantified the following radionuclides and corresponding gamma transitions: ^{40}K (1460.8 keV), ^{208}Tl (583.2, 860.6 and 2614.5 keV), ^{212}Pb (238.6 keV), ^{214}Pb (242, 295.2 and 351.9 keV), ^{214}Bi (609.3, 1120.3 and 1764.5 keV) and ^{228}Ac (338.3, 911.6 and 969.1 keV). Figure 4 shows typical gamma-ray spectra from sites 2 and 8. The calculated average minimum detectable activity (MDA) for ^{40}K was 2 Bq kg^{-1}, whereas the value for ^{214}Pb, ^{214}Bi, and ^{228}Ac was about 0.5 Bq kg^{-1} (Malczewski et al., 2013).

The consistency of activities calculated for gamma-ray transitions from a given multiline radionuclide (e.g., ^{208}Tl, ^{214}Bi, ^{214}Pb, ^{228}Ac) were checked using a line activity consistency evaluator (LACE) analysis. For all measurements obtained under *in situ* methods, the activity ratios for the multiline radionuclides were close to unity. We interpret the activities as indicative of metamorphic processes and other petrological factors. The spectrometer energy was calibrated using a mixed source ^{155}Eu and ^{22}Na model *ISOXSRCE* provided by Canberra Industries and homogeneously dispersed ^{241}Am, ^{109}Cd, ^{139}Ce, ^{57}Co, ^{60}Co, ^{137}Cs, ^{113}Sn, ^{85}Sr, ^{88}Y, and ^{203}Hg radioisotopes in a silicone resin [certificate source type Marinelli Beaker Standard Source (MBSS) supplied by the Czech Metrological Institute]. Results from *in situ* measurements were compared with those obtained under laboratory conditions. No significant differences were found between the *in situ* and laboratory measurements.

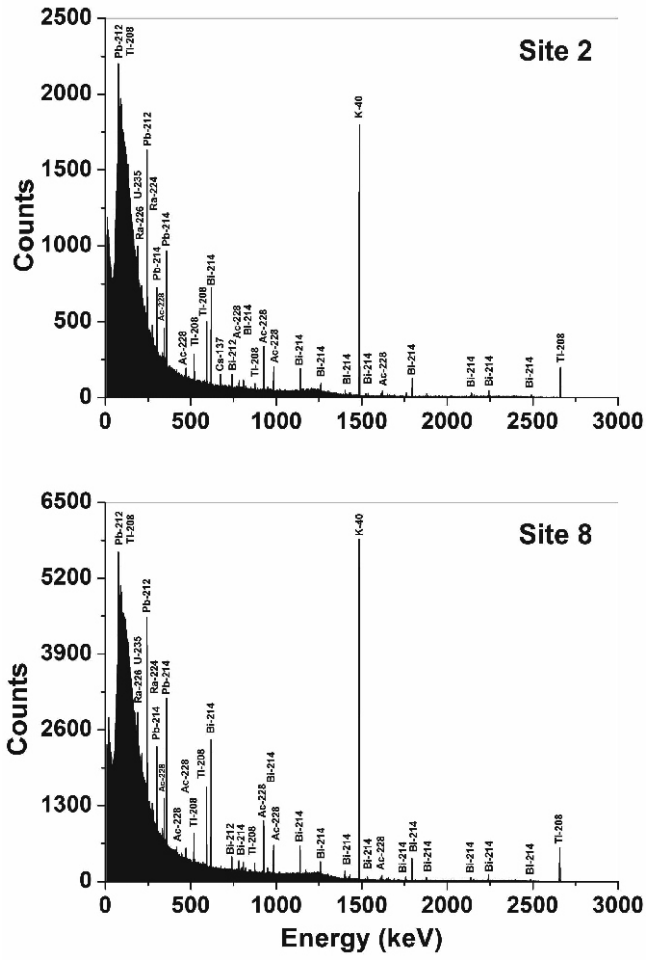

Fig. 4. *In situ* gamma-ray spectra for hornblendite (site 2) and layered gneiss (site 8)

Peaks are labeled to indicate characteristic gamma-ray emitters

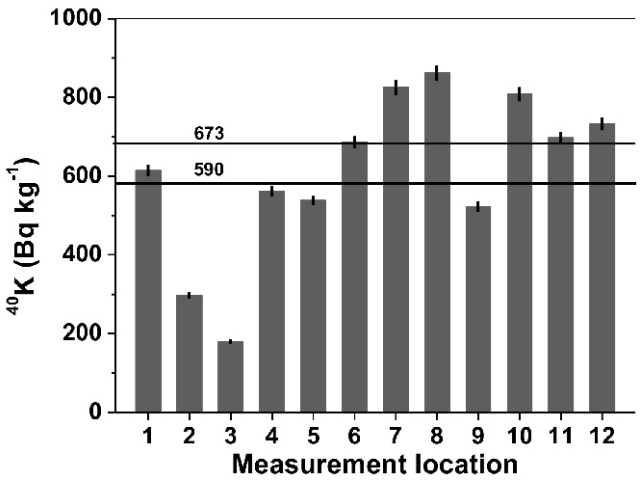

Fig. 5. Activity concentrations for ^{40}K

The thicker black line indicates the average ^{40}K value from all sites, whereas the thinner line shows the average ^{40}K activity value only for gneisses (excluding sites 1, 2 and 3)

RESULTS

Table 1 provides *in situ* activity concentrations for ^{40}K, ^{208}Tl, ^{212}Pb, ^{228}Ac, ^{214}Pb, ^{214}Bi, ^{226}Ra from all 12 measurement sites.

^{40}K

As shown in Figure 5, the sampled sites gave an average ^{40}K activity value of 588 ± 197 Bq kg^{-1}. The arithmetic mean calculated for "pure gneiss" (excluding sites 1, 2 and 3) was 673 ± 121 Bq kg^{-1}. The lowest ^{40}K activity (180 Bq kg^{-1}) was recorded in mylonitic granulite (site 3). This value probably results from ultramafite inclusions within the outcrop. A relatively low ^{40}K activity value of 297 Bq kg^{-1} was noted in hornblendite (site 2). However, the activity still exceeds the 1–7 Bq kg^{-1} range expected for ultramafic rocks (Van Schmus, 1995).

Potassium in hornblende (1–2 wt.% K_2O) and/or that arising from biotization of hornblendite near shear zones may contribute to the observed ^{40}K enrichment. The relatively high granulite ^{40}K activity value (614 Bq kg^{-1}, site 1) confirms the abundance of potassium feldspar in these rocks.

Among the gneiss outcrops the lowest ^{40}K activity concentrations were recorded in homophanized gneiss (508 Bq kg^{-1}, site 5) and layered migmatite (528 Bq kg^{-1}, site 9). The other two migmatic gneiss types gave noticeably higher values of 562 Bq kg^{-1} (site 4) and 686 Bq kg^{-1} (site 6). The substitution of potassium feldspar by sodium feldspar should lead to lower ^{40}K activity values in homophanized and migmatized gneiss relative to other gneiss. Rocks from sites 5 and 9 show evidence of this effect. The higher ^{40}K activity at site 6 likely reflects the abundant biotite and granite veins present in the outcrop.

The highest ^{40}K activity concentrations in this study were observed in layered gneiss at sites 7 and 8 (Walim–Rzeczka complex) where the outcrops emitted concentrations of 826 and 863 Bq kg^{-1}, respectively (mean of 845 Bq kg^{-1}). The outcrops at this locality included typical folded layered gneiss and showed no signs of homophanization. The presence of granite bodies in these outcrops may explain the elevated ^{40}K activity values. Augen gneiss near the Intra-Sudetic Fault is characterized by similar elevated ^{40}K activity (822 Bq kg^{-1}, site 10). Flaser gneiss having a varied degree of homophanization showed ^{40}K activity concentration of 698 Bq kg^{-1} (site 11) and resembled the value observed from migmatic layered gneiss (site 6). Relatively high ^{40}K activity was noted in mylonitic gneiss (733 Bq kg^{-1}, site 12). The elevated value indicates that mylonitization of pre-existing layered and flaser gneiss did not cause potassium migration.

^{232}Th SERIES (^{228}Ac, ^{212}Pb, ^{208}Tl)

As seen in Table 1 radioactive equilibrium is achieved for each rock between progenies in the ^{232}Th series. Since ^{228}Ac is the second radionuclide in the thorium series, the activity of ^{232}Th is assumed to be equal to the ^{228}Ac activity.

The ^{232}Th activity averaged over all sites was 33 ± 12 Bq kg^{-1}, while the average value associated with gneiss (excluding sites 1, 2 and 3) was 39 ± 7 Bq kg^{-1} (Fig. 6). Homophanized and augen gneiss gave the highest ^{232}Th series activity (53 Bq kg^{-1} at site 5 and 48 Bq kg^{-1} at site 10, respectively). Most of the ^{232}Th activity values from the gneiss fell within a narrow range of 32 Bq kg^{-1} (site 6) to 39 Bq kg^{-1} (site 4) (Fig. 6). The homophanization process affecting gneiss at sites 4 and 5 appears to have caused ^{232}Th enrichment.

Mylonitic granulite (site 3), hornblendite (site 2) and granulite (site 1) gave the lowest observed ^{232}Th activity (10, 13 and 24 Bq kg^{-1}, respectively; Fig. 6). The average value of 32 Bq kg^{-1} calculated for all the sites considerably exceeded these values. For hornblendite, the ^{232}Th activity value of 13 Bq kg^{-1}

Table 1

Activity concentrations of primordial radionuclides measured at sample sites

		Activity (Bq kg^{-1})						
Measurement location		^{40}K	^{208}Tl*	^{212}Pb	^{228}Ac	^{214}Pb	^{214}Bi	^{226}Ra$^{\#}$
1	Granulite N = 57°47.007', E = 016°27.542', 288 a.s.l.	614 ± 14	8.7 ± 0.5	23.6 ± 1.0	23.7 ± 1.0	13.8 ± 1.1	13.5 ± 0.6	13.7 ± 1.3
2	Hornblendite N = 57°47.026', E = 016°27.555', 290 a.s.l.	297 ± 7	5.3 ± 0.3	13.4 ± 0.7	13.5 ± 0.8	14.2 ± 1.0	14.6 ± 0.9	14.4 ± 1.4
3	Mylonitic granulite N = 57°47.027', E = 016°27.578', 290 a.s.l.	180 ± 5	3.4 ± 0.3	9.1 ± 0.8	10.0 ± 1.0	8.9 ± 0.8	8.3 ± 0.7	8.6 ± 1.0
4	Migmatic gneiss N = 50°42.524', E = 016°32.723', 354 a.s.l.	562 ± 13	13.7 ± 0.7	37.4 ± 1.3	38.7 ± 1.6	36.7 ± 1.4	37.5 ± 1.5	37.1 ± 2.0
5	Homophanized gneiss N = 50°42.226', E = 016°30.512', 579 a.s.l.	508 ± 12	18.8 ± 1.0	51.8 ± 1.7	52.6 ± 2.0	32.9 ± 1.5	33.2 ± 1.4	33.1 ± 2.1
6	Migmatic layered gneiss N = 50°41.341', E = 016°26.678', 565 a.s.l.	686 ± 16	11.2 ± 0.6	33.3 ± 1.3	32.3 ± 1.3	36.5 ± 1.4	36.3 ± 1.3	36.4 ± 2.1
7	Layered gneiss	826 ± 19	12.7 ± 0.7	35.5 ± 1.5	36.4 ± 1.4	42.9 ± 1.7	43.3 ± 1.4	43.1 ± 2.2
8	Layered gneiss	863 ± 20	13.4 ± 0.7	34.9 ± 1.5	35.8 ± 1.3	42.0 ± 1.7	44.2 ± 1.5	43.1 ± 2.3
9	Layered migmatite N = 50°44.897', E = 016°25.332', 405 a.s.l.	528 ± 12	11.9 ± 0.7	33.0 ± 1.1	32.7 ± 1.3	31.4 ± 1.4	30.8 ± 1.3	31.1 ± 1.9
10	Augen gneiss N = 50°39.796', E = 016°28.855', 423 a.s.l.	822 ± 18	18.4 ± 1.0	49.5 ± 2.1	48.2 ± 1.8	40.4 ± 1.5	41.6 ± 1.6	41.0 ± 2.2
11	Flaser gneiss N = 50°39.201', E = 016°31.121', 791 a.s.l.	698 ± 16	12.8 ± 0.8	36.5 ± 1.1	35.6 ± 1.4	30.3 ± 1.1	29.9 ± 1.3	30.1 ± 1.6
12	Mylonitic gneiss N = 50°34.542', E = 016°38.782', 672 a.s.l.	733 ± 16	13.2 ± 0.7	34.9 ± 1.4	35.4 ± 1.4	21.9 ± 1.3	21.2 ± 1.1	21.6 ± 1.7

* – branching ratio 36%; # – based on ^{214}Pb and ^{214}Bi activities; uncertainties given as 1

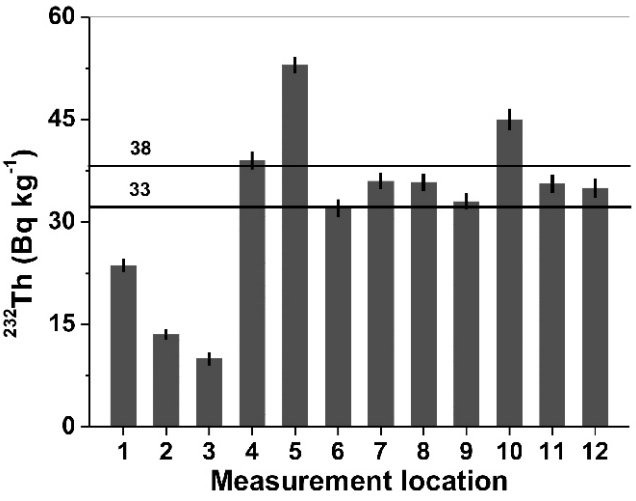

Fig. 6. Measured ^{232}Th activity values

The thicker black line shows the average value from all the rocks whereas the thinner line shows the average activity value from gneisses only (excluding sites 1, 2 and 3)

exceeded the average value of ~10^{-2} Bq kg^{-1} observed from other examples of ultramafic rocks (Van Schmus, 1995).

^{238}U SERIES (^{214}Pb, ^{214}Bi, ^{226}Ra)

Activity concentrations for ^{238}U were estimated by assuming radioactive equilibration of the ^{238}U ^{226}Ra ^{222}Rn ^{214}Pb ^{214}Bi decay chain, an assumption that holds for the great majority of rocks and minerals (Eisenbud and Gesell, 1997; Malczewski and Dziurowicz, 2015). The overlapping of the 186.2 keV (^{226}Ra) and 185.7 keV (^{235}U) gamma peaks along with elevated background noise around this energy range contributes to larger cumulative uncertainties relative to those calculated from averaged ^{214}Pb and ^{214}Bi measurements (Justo et al., 2006; Malczewski and Żaba, 2012). Therefore, in our work we estimated ^{226}Ra (^{238}U) from ^{214}Pb and ^{214}Bi activities.

Figure 7 shows an average ^{238}U activity value of 28 ± 11 Bq kg^{-1} for all sites. Gneiss, (excluding sites 1, 2 and 3) gives an average activity of 34 ± 6 Bq kg^{-1}. An average ^{238}U activity of 32 Bq kg^{-1} with a standard deviation of 12 Bq kg^{-1} for the four rock samples from the Sowie Mountains was reported by Przylibski (2004). The lowest ^{238}U activities were recorded in mylonitic granulite (9 Bq kg^{-1}, site 3), granulite (14 Bq kg^{-1}, site 1) and hornblendite (14 Bq kg^{-1}, site 2). The ^{238}U activity value in hornblendite probably reflects the presence of apatite. As with ^{232}Th observations, five ^{238}U activity values fell within a very nar-

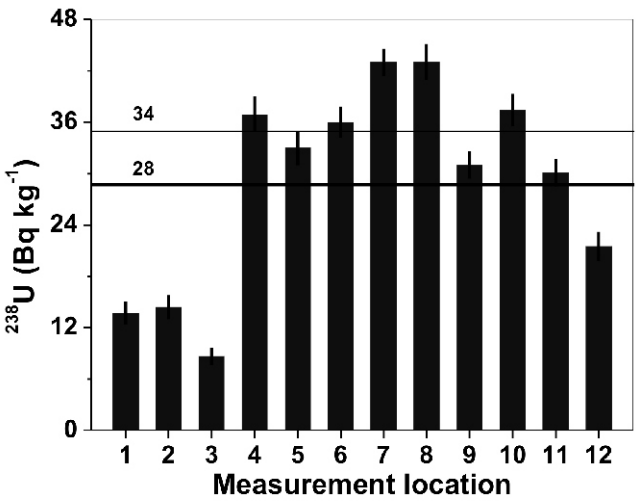

Fig. 7. Measured ^{238}U activity values

The thicker black line shows the average value from all the rocks while the thinner line shows the average activity value from the gneisses only (excluding sites 1, 2 and 3)

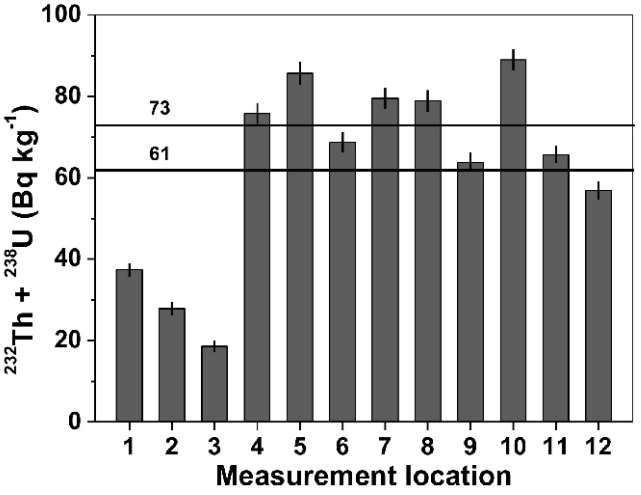

Fig. 8. Combined Th and U activity values

The thicker black line shows the average value from all the rocks, while the thinner line shows the average activity value from the gneisses only (excluding sites 1, 2 and 3)

row range from 30 Bq kg^{-1} (flaser gneiss, site 11) to 37 Bq kg^{-1} (migmatic gneiss, site 4). Slightly elevated ^{238}U activities of 43 Bq kg^{-1} were observed in layered gneiss (sites 7 and 8). Among the gneiss samples, the lowest ^{238}U activity value (22 Bq kg^{-1}) occurred in mylonitic gneiss (site 12). In contrast to its apparent effects on ^{40}K and ^{232}Th values, mylonitization of layered and flaser gneiss appears to diminish uranium concentrations.

DISCUSSION

COMBINED ACTIVITY OF ^{232}Th AND ^{238}U

The average combined Th + U activity for all the rocks investigated was 61 ± 22 Bq kg^{-1}, whereas the average activity for the gneiss only (excluding sites1, 2 and 3) was 73 ± 11 Bq kg^{-1} (Fig. 8). As expected, the lowest combined activities were observed in mylonitic granulite (19 Bq kg^{-1}), hornblendite (28 Bq kg^{-1}) and granulite (37 Bq kg^{-1}). Kresl and Vankova (1982) reported a similar combined Th + U activity value of 39 Bq kg^{-1} for granulite from the Bohemian Massif (Th and U activities of 27 and 12 Bq kg^{-1}, respectively).

Among the gneiss samples analysed here, the lowest Th + U activities are characteristic for mylonitic gneiss (57 Bq kg^{-1}, site 12) and layered migmatite (64 Bq kg^{-1}, site 9). The highest combined activities were obtained for augen gneiss (89 Bq kg^{-1}, site 10) and homophanized gneiss (86 Bq kg^{-1}, site 5). Relative to typical layered migmatite (site 9), homophanization in migmatic gneiss appears to coincide with higher Th + U activity values (sites 4 and 6). Flaser gneiss shows a lower Th + U activity (66 Bq kg^{-1}, site 11) relative to that observed in augen gneiss. As seen in Figure 9, average activity values for ^{40}K, ^{232}Th and ^{238}U in gneiss outcrops from the Sowie Mountains resemble those obtained by similar methods for greywacke and muddy-clay shale found in the quarries of the Opava Mountains (Sudetes, Poland, ~80 km east of the Sowie Mountains) (Dżaluk, 2012). Similarities in these values may indicate that sandy-muddy and muddy-clay shale deposits (or sandy-muddy deposits enriched in clay minerals) comprised the protoliths of the gneiss outcrops analyzed here. The results reported here generally validate interpretations of a sedimentary origin for the majority of the Sowie gneiss. For example, orthogneiss from the Savona Unit (found in the boundary zone between the Alps and Apennines) exhibit ^{40}K, ^{232}Th and ^{238}U activity values of 1340 ± 250, 70 ± 9 and 63 ± 13, respectively (Pasquale et al., 2001).

ESTIMATES OF K (wt.%) ^{232}Th (ppm) AND ^{238}U (ppm)

Activity concentrations of ^{40}K, ^{228}Ac and ^{226}Ra that were measured in outcrops of the Sowie Mountains allowed us to calculate K (wt.%), ^{232}Th (ppm) and ^{238}U (ppm) concentrations (Fig. 10).

The concentration estimates varied in a manner similar to those observed for the activity values. A mylonitic granulite and a hornblendite gave the lowest K contents (0.59 and 0.98 wt.%, respectively), while the highest content occurred in layered gneiss (2.79 wt.%) and augen gneiss (2.71 wt.%). For other localities, the K content ranged from 1.68 wt.% (homophanized gneiss) to 2.42 wt.% (flaser gneiss). The concentration averaged over all the rocks is 1.94 ± 0.65 wt.%, whereas the average for gneiss only is 2.22 ± 0.40 wt.% (Fig. 10). The lowest concentrations of ^{232}Th were calculated for mylonitic granulite and hornblendite (2.5 and 3.3 ppm, respectively). The highest ^{232}Th concentrations were calculated for homophanized gneiss and augen gneiss (12.9 and 11.8 ppm, respectively). For other gneiss, Th concentrations varied within a relatively narrow range from 7.9 ppm (migmatic layered gneiss) to 9.5 ppm (migmatic gneiss). The average ^{232}Th concentration estimated over all sites was 8.0 ± 3.0 ppm (Fig. 10), while the average concentration for gneiss was 9.6 ± 1.7 ppm.

As with the ^{232}Th concentration estimates, the lowest ^{238}U (ppm) concentrations occurred in mylonitic granulite (0.7 ppm), granulite (1.11 ppm) and hornblendite (1.17 ppm). The concentrations of ^{238}U for gneiss (sites 4–12) ranged from 1.74 ppm (mylonitic gneiss) to 3.49 ppm (layered gneiss). The average ^{238}U concentration estimated for all sites was 2.28 ± 0.91 ppm, whereas the average value calculated for gneiss was 2.77 ± 0.52 ppm (Fig. 10).

In the study area, concentrations of K and ^{232}Th that ranged from 0.75 to 1.25% and 4 to 9 ppm, respectively, were reported by previous research (Strzelecki et al., 1994, 2000; Strzelecki and

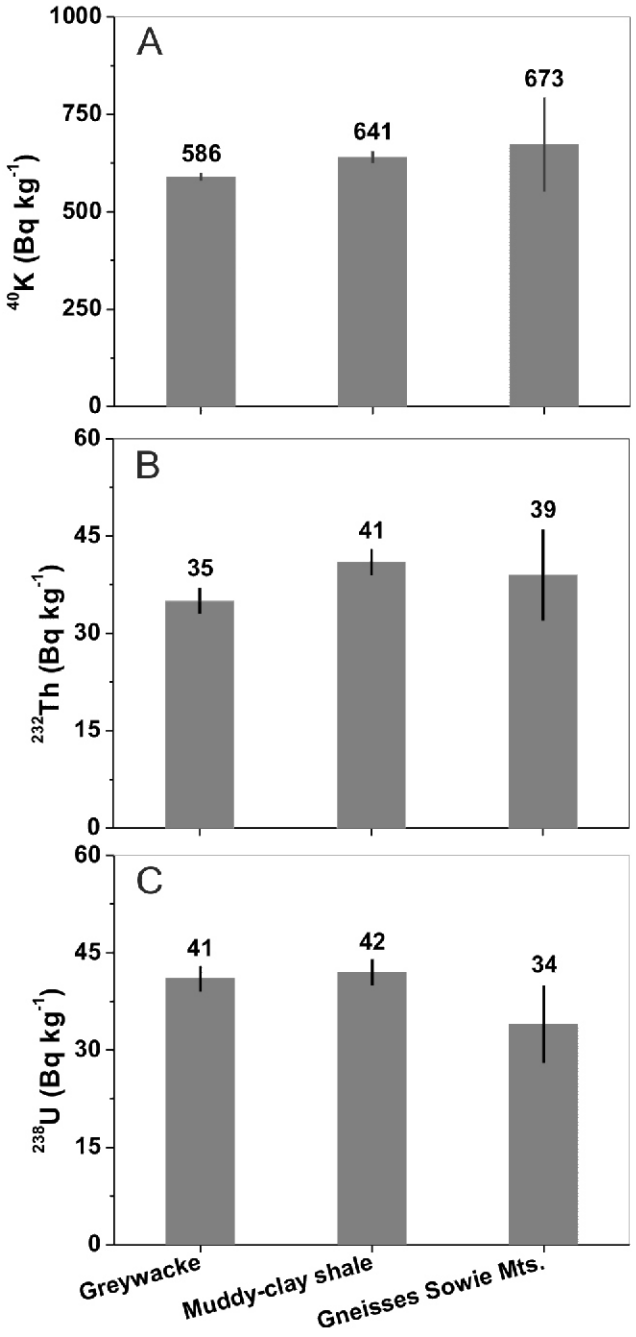

Fig. 9. Average A – ^{40}K, B – ^{232}Th and C – ^{238}U activity values in gneisses of the Sowie Mountains compared with corresponding activities recorded in greywacke and muddy-clay shales of the Opava Mountains

Wołkowicz, 1995). The data were also collected in situ using a scintillation gamma-ray detector. In the same papers measured concentrations of ^{238}U ranged from 1 to 3 ppm.

^{232}Th / ^{238}U RATIOS

Figure 11 shows ^{232}Th/^{238}U concentration ratios for rocks of the Sowie Mountains. The highest ^{232}Th/^{238}U ratios occurred in granulite (5.3), homophanized gneiss (4.8) and mylonitic gneiss (4.5). For other rocks the ratio ranged from ~2.6 in layered

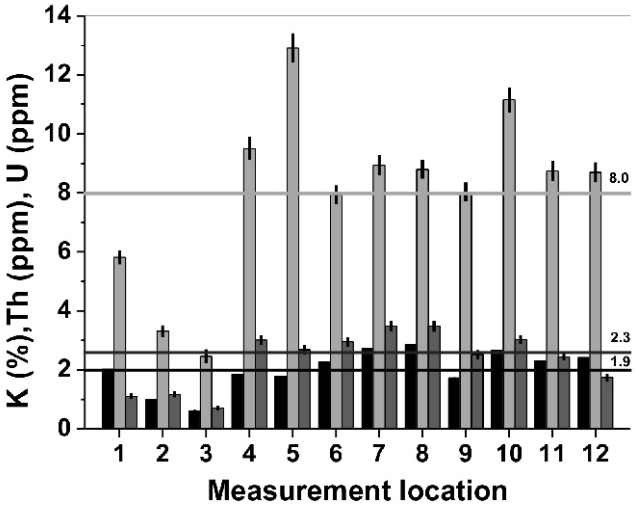

Fig. 10. Estimated concentrations for K (wt.%, black bars), ^{232}Th (ppm, light bars) and ^{238}U (ppm, grey bars)

The horizontal line represents the average value calculated over all units analysed; the following conversion factors were used: K (%) 303.16 = ^{40}K (Bq kg^{-1}); ^{232}Th (ppm) 4.07 = ^{232}Th (Bq kg^{-1}); and ^{238}U (ppm) 12.36 = ^{238}U (Bq kg^{-1}) (Plewa and Plewa, 1992)

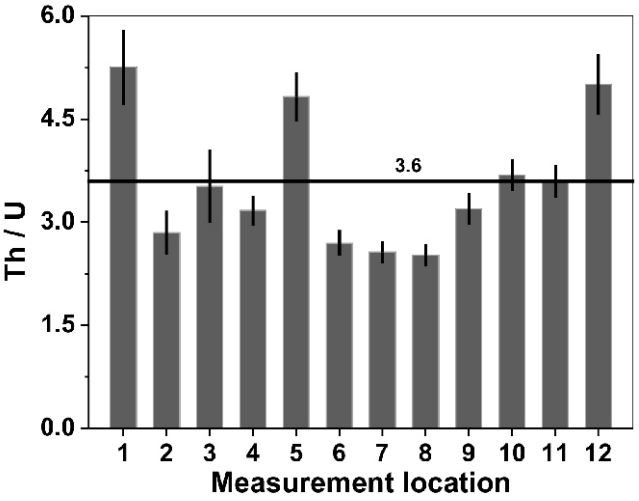

Fig. 11. Calculated ^{232}Th/^{238}U concentration ratios

The horizontal line represents both the average ratio derived from all units and from gneisses alone

gneiss (sites 7 and 8) to 3.5 in mylonitic granulite. An arithmetic mean ^{232}Th/^{238}U value of 3.6 ± 0.9 is the same for gneiss and all lithologies analyzed here. For the gneiss, the average Th/U ratio of 3.6 falls within the 3.5–4 range reported for biotite gneiss (Kresl and Vankova, 1978; Plewa and Plewa, 1992) but is lower than the 4.3–5.7 range reported for typical granites (Van Schmus, 1995; Eisenbud and Gesell, 1997).

Comparison of K (wt.%), ^{232}Th (ppm) and ^{238}U (ppm) concentrations with values reported for gneiss from other locations

Figures 12 and 13 compare K, Th and U values reported here with those obtained using similar *in situ* field methods for gneiss from Gebel Me'atiq (Egypt; Abd El Nabi, 2013), gneiss from the Izera Mountains (Sudetes, Poland; Malczewski et al.,

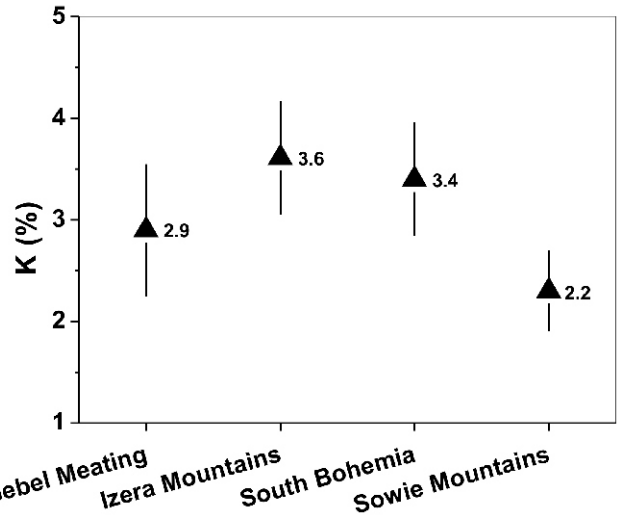

Fig. 12. Comparison of K content (wt.%) among the gneisses of the Sowie Mountains and from other locations

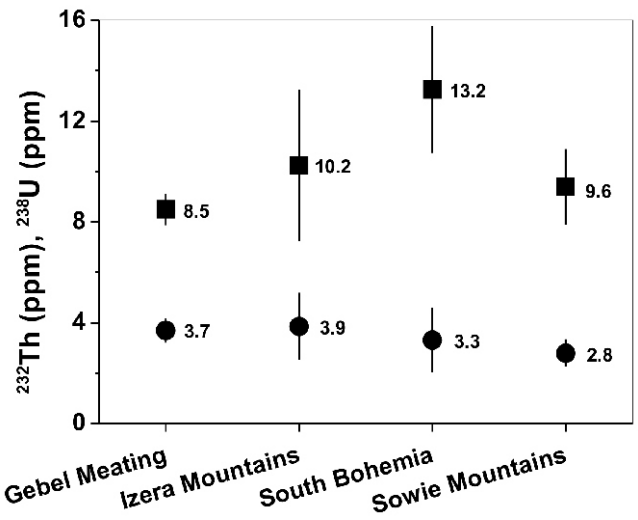

Fig. 13. Comparison of Th (squares) and U (circles) concentrations (ppm) among gneisses from the Sowie Mountains and from other locations

2004, 2005) and from laboratory measurements analyzing biotite gneiss from the Bohemian Massif (Czech Republic; Kresl and Vankova, 1978).

Figure 12 shows that average K content in gneiss from the Sowie Mountains (2.2 wt.%) coincides with that from Gebel Me'atiq (2.9 wt.%). The values for K content in gneiss from the Izera Mountains (3.5 wt.%) and Bohemian Massif (3.4 wt.%) exceed those observed in the Sowie Mountains.

The average ^{232}Th concentration estimated for gneiss from the Sowie Mountains (9.6 ppm) also resembles those estimated for units in Gebel Me'atiq (8.5 ppm) and the Izera Mountains (10.5 ppm). Laboratory measurements for ^{232}Th concentrations in gneiss from the Bohemian Massif gave an average value of 13.2 ppm. The average ^{238}U (ppm) concentration estimated for the gneiss from the Sowie Mountains (2.8 ppm) was lower than that reported for gneiss from Gebel Me'atiq (3.7 ppm), the Izera Mountains (3.9 ppm) and Bohemian Massif units (3.3 ppm; Fig. 13).

CONCLUSIONS

In situ measurements of ^{40}K, ^{232}Th and ^{238}U activity for gneiss found in the Sowie Mountains are similar to the values recorded from muddy-clay shale and greywacke. The similarity in these values indicates that the gneiss is probably paragneiss. Homophanized and augen gneiss samples showed noticeably higher Th and U activity values. The elevated ^{232}Th values and lower ^{40}K values in homophanized gneiss appear to be associated with Carboniferous granitoid magmatism. Augen gneiss samples showed the highest combined Th + U activity and elevated ^{40}K activity, indicating a significant contribution from igneous activity along the Intra-Sudetic Fault.

Acknowledgements. We thank three unknown reviewers for critical comments that improved the final version of this paper.

REFERENCES

Abd El Nabi, S.H., 2013. Role of gamma-ray spectrometry in detecting potassic alteration associated with Um Ba'anib granitic gneiss and metasediments, G. Meatiq area, Central Eastern Desert, Egypt. Arabian Journal of Geosciences, **6**: 1249–1261.

Aleksandrowski, P., Mazur, S., 2002. Collage tectonics in the northeasternmost part of the Variscan Belt: the Sudetes, Bohemian Massif. Geological Society Special Publications, **201**: 237–277.

Aleksandrowski, P., Kryza, R., Mazur, S., Żaba, J., 1997. Kinematic data on major Variscan strike-slip faults and shear zones in the Polish Sudetes, northeast Bohemian Massif. Geological Magazine, **134**: 727–739.

Bakun-Czubarow, N., 1981. Ultrabasic rocks in granulites of the Góry Sowie Mts. Block. In: Ophiolites and Initialites of Northern Border of the Bohemian Massif (ed. W. Narębski): 79–86. Wissenschaftlichen Informationzentrums des Bergakademic Freiberg, Potsdam Freiberg.

Bröcker, M., Żelaźniewicz, A., Enders, M., 1998. Rb-Sr and U-Pb geochronology of migmatitic gneisses from the Góry Sowie (West Sudetes, Poland): the importance of Mid-Late Devonian metamorphism. Journal of the Geological Society, **155**: 1025–1036.

Cwojdziński, S., 1980. Geologic evolution of South-Western Poland interpreted in terms of plate tectonics (in Polish with English summary). Geologia Sudetica, **15**: 43–66.

Cymerman, Z., Piasecki, M.A.J., Seston, R., 1997. Terranes and terrane boundaries in the Sudetes, northeast Bohemian Massif. Geological Magazine, **134**: 717–725.

Dżaluk, A., 2012. Natural radioactivity in rocks of the Opava Mountains (in Polish). MSc. thesis. University of Silesia, Katowice.

Eisenbud, M., Gesell, T., 1997. Environmental Radioactivity from Natural, Industrial, and Military Sources. Academic Press, San Diego.

Grocholski, W., 1967. Structure of the Sowie Mts. (in Polish with English summary). Geologia Sudetica, **3**: 181–249.

Grocholski, W., 1968. Mapa geologiczna Gór Sowich w skali 1:30 000 (in Polish). Polish Academy of Sciences, Wyd. Geol., Warszawa.

Gunia, P., 1997. Petrology of ultrabasic rocks of the Góry Sowie Block. Acta Universitatis Wratislaviensis, **2012** (65): 1–92.

Gunia, T., 1999. Microfossils from the high-grade metamorphic rocks in the Góry Sowie Mts. (Sudetes area) and their stratigraphical importance. Geological Quarterly, **43** (4): 519–536.

Helfer, I.K, Miller, K.M., 1988. Calibration factors for Ge detectors used for field spectrometry. Health Physics, **55**: 15–29.

Janeczek, J., Kozłowski, K., Żaba, J., 1994. Ultramafic rocks from Bystrzyca Górna, Góry Sowie Block: geological position, structure and petrology. In: Igneous Activity and Metamorphic Evolution of the Sudetes Area (ed. R. Kryza): 51–54. Wydawnictwo Uniwersytetu Wrocławskiego, Wrocław.

Justo, J., Evangelista, H., Paschoa, A.S., 2006. Direct determination of ^{226}Ra in NORM/TENORM matrices by gamma-spectrometry. Journal of Radioananlytical and Nuclear Chemistry, **269**: 733–737.

Kresl, M., Vankova, V., 1978. Radioactivity and heat production data from several boreholes in the Bohemian Massif. Studia Geophysica et Geodaetica, **22**: 166–176.

Kresl, M., Vankova, V., 1982. A method of reducing the disturbing effects in gamma-spectrometric measurements of rock radioactivity. Studia Geophysica et Geodaetica, **26**: 67–73.

Kryza, R., 1981. Migmatization in gneisses of northern part of the Sowie Góry, Sudetes (in Polish with English summary). Geologia Sudetica, **14**: 7–100.

Kryza, R., Fanning, C.M., 2007. Devonian deep-crustal metamorphism and exhumation in the Variscan Orogen: evidence from SHRIMP zircon ages from the HT-HP granulites and migmatites of the Góry Sowie (Polish Sudetes). Geodinamica Acta, **20**: 159–175.

Kryza, R., Pin, C., 2002. Mafic rocks in a deep crustal segment of the Variscides (the Góry Sowie, SW Poland): evidence for crustal contamination in an extensional setting. International Journal of Earth Sciences, **91**: 1017–1029.

Kryza, R., Pin, C., Vielzeuf, D., 1996. High-pressure granulites from the Sudetes (south-west Poland): evidence of crustal subduction and collisional thickening in the Variscan Belt. Journal of Metamorphic Geology, **14**: 531–546.

Malczewski, D., Dziurowicz, M., 2015. ^{222}Rn and ^{220}Rn emanations as a function of the absorbed á-doses from select metamict minerals. American Mineralogist, **100**: 1379–1385.

Malczewski, D., Żaba, J., 2012. Natural radioactivity in rocks of the Modane-Aussois region (SE France). Journal of Radioanalytical and Nuclear Chemistry, **292**: 123–130.

Malczewski, D., Teper, L., Dorda, J., 2004. Assessment of natural and anthropogenic radioactivity levels in rocks and soils in the environs of Świeradów Zdrój in Sudetes, Poland, by in situ gamma-ray spectrometry. Journal of Environmental Radioactivity, **73**: 233–245.

Malczewski, D., Żaba, J., Sitarek, A., Dorda, J., 2005. Natural radioactivity of selected crystalline rocks of the Izera Block (Sudetes, SW Poland) (in Polish with English summary). Przegląd Geologiczny, **53**: 237–244.

Malczewski, D., Kisiel, J., Dorda, J., 2013. Gamma background measurements in the Boulby Underground Laboratory. Journal of Radioanalytical & Nuclear Chemistry, **298**: 1483–1489.

Matte, Ph., Maluski, H., Rajlich, P., Franke, W., 1990. Terrane boundaries in the Bohemian Massif: results of large-scale Variscan shearing. Tectonophysics, **177**: 151–170.

Mehnert, K.R., 1968. Migmatites and the Origin of Granitic Rocks. Elsevier, Amsterdam.

Mehnert, K.R., 1971. Migmatites and the Origin of Granitic Rocks. Elsevier, Amsterdam.

Narębski, W., Wajsprych, B., Bakun-Czubarow, N., 1982. On the nature, origin and geotectonic significance of ophiolites and related rock suites in the Polish part of the Sudetes. Ofioliti, **2**: 407–428.

Oberc, J., Badura, J., Przybylski, B., Jamrozik, L., 1994. Mapa geologiczna Polski, ark. Bardo Śląskie, skala 1:25 000 (in Polish). Państwowy Instytut Geologiczny, Warszawa.

O'Brien, P.J., Kröner, A., Jaeckel, P., Hegner, E., Żelaźniewicz, A., Kryza, R., 1997. Petrological and isotopic studies on high-pressure granulites, Góry Sowie Mts., Polish Sudetes. Journal of Petrology, **38**: 433–456.

Pasquale, V., Verdoya, M., Chiozzi, P., 2001. Radioactive heat generation and its thermal effects in the Alps–Apennines boundary zone. Tectonophysics, **331**: 269–283.

Pacholska, A., 1978. On the tectonic breccias at southern edge of the Sowie Góry gneiss block (in Polish with English summary). Geologia Sudetica, **13**: 41–63.

Pin, C., Vielzeuf, D., 1983. Granulites and related rocks in Variscan median Europe: a dualistic interpretation. Tectonophysics, **93**: 47–74.

Plewa, M., Plewa, S., 1992. Petrofizyka (in Polish). Wyd. Geol., Warszawa.

Polański, A., 1955. On the metamorphism of crystalline formations of the Sowie Góry Mts. (Middle Sudetes) (in Polish with English summary). Archiwum Mineralogiczne, **18**: 211–284.

Przylibski, T.A., 2004. Concentrations of ^{226}Ra in rocks of the southern part of Lower Silesia (SW Poland). Journal of Environmental Radioactivity, **75**: 171–191.

Quenardel, M.J., Brochwicz-Lewiński, W., Chorowska, M., Cymerman, Z., Grocholski, A., Kossowska, I., Pique, A., Ploquin, A., Santallier, D., 1988. The Polish Sudetes: a mosaic of Variscan terranes. Trabajos de Geologia Universidad Oviedo, **17**: 139–144.

Sachanbiński M., 1973. Apatite mineralization at Bystrzyca Górna (Sudetes Mts) (in Polish). Przegląd Geologiczny, **20**: 401–402.

Strzelecki, R., Wołkowicz, S., 1995. Maps of radioactive elements (in Polish with English summary). In: Geochemical Atlas of Poland 1:2 500 000 (eds. J. Lis and A. Pasieczna). Państwowy Instytut Geologiczny, Warszawa.

Strzelecki, R., Wołkowicz, S., Szewczyk, J., Lewandowski, P., 1994. Mapa radioekologiczna Polski. Część II. Mapy zawartości uranu, toru i potasu w Polsce (in Polish). Państwowy Instytut Geologiczny, Warszawa.

Strzelecki, R., Wołkowicz, S., Nałęcz, T., 2000. Radioactive elements and radioecological hazard in towns of the Sudetic region (SW Poland) (in Polish with English summary). Przegląd Geologiczny, **48**: 1139–1150.

Van Breemen, O., Bowes, D.R., Aftalion, M., Żelaźniewicz, A., 1988. Devonian tectonothermal activity in the Sowie Góry gneissic block, Sudetes, south western Poland: evidence from Pb-Sr and U-Pb isotopic studies. Annales Societatis Geologorum Poloniae, **58**: 3–19.

Van Schmus, W.R., 1995. Natural radioactivity of the crust and mantle. In: Global Earth Physics (ed. T.J. Ahrens). American Geophysical Union, Washington.

Vielzeuf, D., Pin, C., 1989. Geodynamic implications of granulitic rocks in the Hercynian belt, In: Evolution of metamorphic belts. Geological Society Special Publications, **43**: 343–348.

Winchester, J.A., Floyd, P.A., Awdankiewicz, M., Piasecki, M.A.J., Awdankiewicz, H., Gunia, P., Gliwicz, T., 1998. Geochemistry and tectonic significance of metabasic suites in the Góry Sowie Block, SW Poland. Journal of the Geological Society, **155**: 155–164.

Żakowa, H., 1966. Zone Goniatites crenistria phill. in the vicinity of Sokolec and Jugów, at the foot of the Sowie Góry Mountains (Central Sudetes) (in Polish with English summary). Prace Instytutu Geologicznego, **43**: 1–197.

Żelaźniewicz, A., 1985. Granulitic inliers amidst a geneissic-migmatitic complex of the Owl Mts., Sudetes. Acta Geologica Polonica, **35**: 157–171.

Żelaźniewicz, A., 1987. Tectonic and metamorphic evolution of the Góry Sowie, Sudetes Mts., SW Poland (in Polish with English summary). Annales Societatis Geologorum Poloniae, **57**: 203–348.

Żelaźniewicz, A., Aleksandrowski, P., Buła, Z., Karnkowski, P.H., Konon, A., Oszczypko, N., Ślączka, A., Żaba, J., Żytko, K., 2011. Regionalizacja tektoniczna Polski (in Polish). Polish Academy of Sciences, Wrocław.